Published in final edited form as:
Clin Neurophysiol. 2008 February ; 119(2): 388–398.

Magnetic sources of the M50 response are localized to frontal cortex

E. Garcia-Rill[*], **K. Moran**, **J. Garcia**, **W. M. Findley**, **K. Walton**, **B. Strotman**[*], and **R. R. Llinas**
Department of Neuroscience and Physiology, New York University School of Medicine, New York, NY

[*]*Center for Translational Neuroscience, Dept. Neurobiology & Dev. Sci.,University of Arkansas for Medical Sciences, Little Rock, AR*

Abstract

Objective: To determine the source localization(s) of the midlatency auditory magnetic response M50, the equivalent of the P50 potential, a sleep state-dependent waveform known to habituate to repetitive stimulation.

Methods: We used a paired stimulus paradigm at interstimulus intervals of 250, 500 and 1,000 msec, and magnetoencephalographic (MEG) recordings were subjected to computational methods for current density reconstruction, blind source separation, time-frequency analysis, and data visualization to characterize evoked dynamics.

Results: Each subject showed localization of a source for primary auditory evoked responses in the region of the auditory cortex, usually at a 20-30 msec latency. However, responses at 40-70 msec latency that also decreased following the second stimulus of a pair, were not localizable to the auditory cortex, rather showing multiple sources usually including the frontal lobes.

Conclusions: The M50 response, which shows habituation to repetitive stimulation, was not localized to the auditory cortex, but showed multiple sources including frontal lobes.

Significance: These MEG results suggest that sources for the M50 response may represent non-auditory, perhaps arousal-related, diffuse projections to the cortex.

Keywords

auditory evoked responses; magnetoencephalography; P50 potential

Introduction

Early electroencephalographic (EEG) work based on topographical studies of human auditory evoked potentials concluded that auditory evoked potentials in the 20-60 msec latency range were generated in the posterior temporal lobe (Vaughan and Ritter, 1970; Wood and Wolpaw, 1982), however, other workers found the P50 potential still to be present after bilateral lesions of the temporal lobe (Woods et al., 1984). Another study concluded that the source for the P50 potential was indeed the temporal lobe, but could not exclude the contribution of other sources

Corresponding author: E. Garcia-Rill, PhD, Professor and Director Center for Translational Neuroscience Dept. Neurobiology & Dev. Sci. University of Arkansas for Medical Sciences 4301 West Markham St., Slot 847 Little Rock, AR 72205 GarciaRillEdgar@uams.edu Tel. 501-686-5167; fax 501-526-7928.

(Reite et al., 1988). Some studies that reported cortical localization used inappropriate parameters such as 50-100 msec stimuli that outlasted the initial response (Godey et al., 2001; Onitsuka et al., 2003), or stimulation at too high a frequency (Makela et al., 1994; Yoshiura et al., 1995), which leads to habituation of the P50 potential (Erwin and Buchwald, 1987). Perhaps the most telling early study involved surface and depth recordings in human subjects (Goff et al., 1980). Depth recording electrodes passing vertically and medially to the primary auditory cortex on the superior temporal gyrus failed to find a reversal across the Sylvian fissure, as did electrodes passing along the long axis of the temporal lobe from the occipital cortex to the tip of the temporal lobe. These authors concluded that their data "failed to select from the two theories" on the origin of this potential (Goff et al., 1980), the temporal auditory cortex vs a modality nonspecific response (Williamson et al., 1970).

Studies by Buchwald demonstrated the labile nature of the P50 potential (state-dependence, rapid habituation at frequencies >1 Hz, and blockade by non-soporific doses of scopolamine), in contrast to the robust nature of the primary auditory cortex Pa potential (at a 25 msec latency) generated by the primary auditory cortex (that is present during all sleep-wake states, failed to habituate at high frequencies of stimulation and was unaffected by scopolamine) (Erwin and Buchwald, 1986a, b). The sleep state-dependence of the P50 potential was confirmed by others (Kevanishvili and von Specht, 1979). While the source of the Pa potential has been localized to the primary auditory cortex in the posterior temporal lobe, the nature of the P50 potential, Buchwald argued, was more consistent with waveforms generated by the reticular activating system (RAS) (Erwin and Buchwald, 1986a, b). Work on animal equivalents of the P50 potential (Garcia-Rill and Skinner, 2002), lends further support to the probable involvement of brainstem sources of this waveform, at least in part.

A key element in P50 potential manifestation is its habituation to repetitive stimulation. Many studies have used the P50 potential to study habituation, a component of the process of sensory gating, the ability to filter incoming information in order to attend to salient stimuli. Normal subjects show a markedly lower response to the second of closely spaced stimuli (Erwin and Buchwald, 1986a, Boutros and Belger, 1999), however, decreased habituation of the P50 potential has been reported in schizophrenia (Adler et al., 1982), autism (Buchwald et al., 1992), narcolepsy (Boop et al., 1994), post traumatic stress disorder (Skinner et al., 1999), Parkinson's Disease (Teo et al., 1997), Huntington's Disease (Uc et al., 2002) and depression (Garcia-Rill et al., 2002). A comprehensive study using depth recordings in epilepsy patients with electrodes implanted in the hippocampus and parahippocampal gyrus found "no P50-like activity within the hippocampus in any of our subjects" (Grunwald et al., 2003). Using subdural electrodes for cortical recordings, these authors observed responses at ~50 msec latency that habituated to repetitive stimulation in only 6/24 patients, and these were confined to prefrontal cortex and temporo-parietal regions near, but not in the primary auditory cortex (Grunwald et al., 2003). As such, the P50 potential appears to represent, rather than a primary auditory response, a preattentive process useful for the study of a number of conditions that manifest arousal/preattentive deficits. Given that a number of these disorders show MEG abnormalities in the form of thalamocortical dysrhythmia (Llinas et al., 2002), it is important to determine the characteristics of the magnetic equivalent of the P50 potential.

In terms of the P50 EEG vs the M50 MEG response, one study failed to localize a specific auditory M50 response using MEG (Yvert et al., 2005), while another reported clear differences between the P50 and M50 responses in responses to cholinergic agents (Pekkonen et al., 2005). These reports suggest that, based only on latency (without regard for habituation), the originally described characteristics of the P50 potential remain unexplained and suggest a contribution from a subcortical cholinergic source related to arousal level or state, however, the source of the M50 remains to be established. A recent study interpreted both EEG (P50) and MEG (M50) data based on habituation to repetitive stimuli (at a single intertrial interval),

concluding that the two measures may be unrelated and that additional generators may contribute to the P50 potential (Edgar et al., 2003). This study, however, assumed a superior temporal gyrus source for the M50 and used click stimuli only 35 dB above threshold, which may generate little activation of the RAS. Another recent MEG study used unilateral stimulation but at 2.7 and 3.3 Hz, which would cause rapid habituation of RAS responses. These authors described small sources at ~50 msec in the planum temporale, but not in Heschl's gyrus (Inui et al., 2006). This 38-channel instrument is unlikely to detect sources in frontal regions, especially in the region of the vertex where the P50 potential is at its highest amplitude.

The present study was designed to use MEG recordings of responses to appropriate auditory paired stimuli at ~25 and ~50 msec latencies subjected to state-of-the-art computational methods for current density reconstruction, blind source separation, time-frequency analysis, and data visualization to characterize evoked dynamics. The hypothesis tested was that, unlike the primary evoked Pa potential, the magnetic equivalent of the P50 potential undergoing habituation to repetitive stimuli would not be localized to the primary auditory cortex. Of particular interest was the localization of a response at ~50 msec latency that would undergo a decrease in amplitude as the interstimulus interval decreased, i.e. showed a recovery curve similar to that of the P50 potential (Garcia-Rill and Skinner, 2002). Preliminary results have been presented in abstract form (Garcia-Rill et al., 2006).

Methods

Normal subjects aged 24-57, with an group average of (mean ± S.E.) 29±3 years, were composed of 5 females (26±1 years) and 9 males (31±3 years) who were tested after securing informed consent according to procedures approved by the institutional review board. Continuous whole-head cortical activity was recorded with a 148-channel MEG system (4D Imaging, San Diego, CA) at a sampling rate of 508.6 Hz, as previously described (Llinas et al., 1999). Recordings were performed during three conditions in a supine position while subjects' eyes were closed. Subjects were instructed to remain still and alert during the recording. A program was developed on EEGLAB MatLab software to send a TTL pulse to a magnetically silent sound generator connected to plastic tubing terminating in soft earplugs. Auditory stimulation consisted of binaurally administered 20 msec duration tones of 1 kHz paired at interstimulus intervals (ISI) of 250, 500 or 1,000 msec, with an intertrial interval of 5±0.2 sec at 50 dB above threshold. The second stimulus of a pair was the usual 1 kHz tone in the 64/80 trials in a block, but randomly administered as a 2 kHz tone in 16/80 trials. Subjects were asked to count the number of times the second stimulus was different from the first, basically requiring a same-different discrimination to maintain vigilance. All 80 trials were acquired to yield measures in the No Response condition at each of the ISIs. In a variation of this paradigm, instead of the 1,000 msec ISI, some subjects underwent a block of trials using the 250 msec ISI in which they were asked to press a button when the two stimuli were the same (64/80 trials) and to abstain from pressing when they were different (randomly administered in 16/80 trials). This block was designed to provide an additional attentional component to the task by using a go-no go, same-different, response paradigm. All 80 trials were acquired to yield a measure in the Response condition at 250 msec ISI for comparison with the No Response condition previously acquired using the same ISI. In order to limit the total recording time (to prevent fatigue), all subjects were studied only in three blocks of trials each lasting about 15 min. Therefore, some subjects were studied in all three ISIs and others in the Response tasks (see “n” for each condition).

MEG recordings were analyzed as follows. The time-series data was preprocessed so that the magnetic field of each sensor was DC offset by subtracting its mean. Noisy sensors were removed based on overall power and power in relation to near-neighbor channels. The offset data were analyzed using the Infomax independent component analysis (ICA) algorithm

(EEGLAB) to isolate independent components (ICs) (Makeig et al., 1997; Brown et al., 2001). The resulting data set separated into statistically independent activation functions and the accompanying sensor maps revealed the field that each source generated. On average, there were two noisy sensor channels, allowing ICA to provide 146 ICs. The forward model was solved using a spherically symmetric volume conductor head model to compute the leadfields for each subject. A volumetric sourcespace was constructed of averaged MRI (constructed from MNI-152), and voxels with gray matter probability higher than 0.4 were selected. The probabilistic sourcespace was transformed onto a subject-specific head-centered coordinate system and scaled. Using a recursively weighted minimum norm algorithm, current source density estimates were calculated for each sensor map of selected ICs. Current densities were displayed on segmented and inflated cortical surfaces from the averaged MRI processed in FreeSurfer (Fischl et al., 1999; Fischl et al., 2002), referred to here as inflated maps. The event related spectral perturbation (ERSP) (i.e., the spectral power modulation induced by the stimulus indicating evoked activity) and the inter-trial coherence (ITC) (i.e., phase-locking factor indicating synchronization of oscillations) of each selected independent component was computed (Makeig et al., 2002) with the EEGLAB MatLab Toolbox (Delorme and Makeig, 2004) and our own software extensions. The statistical confidence intervals were obtained from surrogate pre-stimulus baseline data using Bootstrapping (Delorme and Makeig, 2004).

Localization of magnetic sources on inflated brain maps was used first to determine whether or not there were sources localized to the primary auditory cortex in the superior temporal gyrus. A source on either the left and/or right superior temporal gyrus was assumed to represent activation of the primary auditory cortex. The ERSP revealed variable activation and deactivation in the 20-30 msec latency range of the Pa potential and in the 40-70 msec latency range of the P50 potential. The ITC for each of the sources was studied to determine if activation occurred in the 20-30 msec latency range. If a source was localized to the primary auditory cortex and there was ITC activation at 20-30 msec latency after either the first or second stimulus of a pair, this was assumed to be the magnetic equivalent of the Pa potential. If the source localized to the primary auditory cortex but there was no ITC activation at ~25 msec, this was tentatively labeled as a magnetic equivalent of the Pa potential. The localization of the magnetic equivalent of the P50 potential was based on a) the presence of ITC activation at a 40-70 msec latency after the first stimulus, and b) the presence of equal or reduced ITC activation at a 40-70 msec latency after the second stimulus, indicative of habituation to repetitive stimulation. If both of these criteria were met, then the inflated maps were searched for ICs of the magnetic equivalent of the P50 potential.

The ERSPs and ITCs of ICs were plotted across 450 msec, beginning 175 msec before the stimulus and ending 275 msec after the stimulus, thus spanning a pre-stimulus baseline and over 200 msec post-stimulus. Two ERSPs and ITCs per IC were plotted to visualize the response after the first and after the second stimulus. In order to quantify changes in ERSP and ITC across subjects and conditions, plots were analyzed by an integrated optical density (IOD) measure to determine the density of the ERSP or ITC induced. Plots were converted to a gray scale (0-255 levels) making sure images were identically sized and had an identical threshold of 200, allowing quantitation across 200-255 gray levels. A calibrated region of interest (ROI) at the 40-70 msec latency range of the P50 potential was measured following the first and second stimuli to quantify the density of the ERSP and ITC at all frequencies by using a summation of all gray values above threshold of individual pixels within the ROI. The IOD measures for the 40-70 msec region was subdivided into 0-10, 10-20, 20-30, 30-40, and >40 Hz areas in order to determine density changes across frequencies of ERSP and ITC. In order to compare the ROIs after the first and second stimuli in the Response vs the No Response condition, the display was expanded to 950 msec, including a 175 msec pre-stimulus baseline, and a 775 msec window that included both first and second stimuli. The density measures of these windows were limited to two 40-70 msec windows after each stimulus, so that the total

ROI was of significantly lower area and, therefore, pixel values than when measuring the individual stimulus windows in the initial analysis of three ISIs described above. Density measures were carried out by two different individuals who did not participate in the recordings and were blind to condition.

Comparisons of ERSP and ITC density in response to the first stimulus of a pair were performed with repeated measures analysis of variance (RM ANOVA), as were comparisons of ERSP and ITC density in response to the second stimulus as a percent of the first across the three ISIs. Also, the ERSP and ITC density in response to the second stimulus of a pair in the Response vs No Response condition were compared.

Results

M50 Localization

Localization of the M50 response was based on a search of the ERSPs and ITCs induced in individual ICs at ~50 msec latency after the first and second stimulus in the 250, 500 and 1,000 msec ISIs for each subject. ERSPs at 40-70 msec latency in the 250 msec ISI were evident in only 3/14 subjects after the first stimulus, and in 3/14 subjects after the second stimulus (2 of these were on the same subjects, i.e. only 2/14 subjects showed ERSPs after both stimuli). ERSPs at a 40-70 msec latency in the 500 msec ISI were present in 5/12 subjects after the first stimulus and in 4/12 after the second (3/12 were on the same subjects), while ERSPs were evident at the same latency in the 1,000 msec ISI in 2/6 subjects after the first and second stimuli (1 on the same subject). ERSP changes induced by the stimuli were, therefore, not present in a majority of subjects at any ISI. The densities of the ERSPs in cases when it was induced were too few for statistical comparisons to be made. On the other hand, every subject (14/14) exhibited at least one IC with ITC activation at a 40-70 msec latency after the first stimulus, and also an equal or reduced ITC activation at a 40-70 msec latency after the second stimulus, suggestive of habituation to repetitive stimulation. Figure 1A shows a representative 64 trial average of the ITC induced by stimuli at the 250 msec ISI in one subject, along with the event related potential after each stimulus. The superimposed individual waveforms shown are from a sensor in the posterior frontal lobe. Note that every subject reliably showed this type of ITC response, namely a large amplitude response following the first stimulus followed by a lower amplitude response after the second stimulus (Fig. 1B). The M50 sources calculated for the ITCs were present in frontal, and impinged on parietal, cortex (Fig. 1C). In 4/14 subjects, there were two ICs showing such characteristics, and in 2/14 subjects, there were three ICs showing M50-like responsiveness. The ITC density was measured in subjects that had more than one M50-like IC, and the highest density (pixel gray values) measured was chosen as that subject's M50 response IC. Figure 2 shows the IC for a representative subject with ERSP induced ITC following the first stimulus at ~50 msec latency, and a reduced density ITC following the second stimulus, also at ~50 msec latency (Fig. 2 A, C). No activation was observed at ~25 msec in either IC. The inflated maps for these ICs showed that the sources were localized to the parietal and frontal lobe in each case, with no activation in the region of the auditory cortex (Fig. 2 B, D). Localization of the M50 in the frontal lobe was present in 11/14 subjects, and in the occipital lobe in 3/14. In 9/14 subjects, additional sources were evident in the occipital, parietal and anterior temporal lobe. That is, in a majority of subjects, localization of the M50 included the frontal and at least one other lobe.

M50 Integrated Optical Density (IOD) measures-initial activation of ITC

The mean IOD following the first stimulus was calculated for subjects tested at the 250 msec (n=14), 500 msec (n=12) and 1,000 msec (n=6) ISIs. These IOD means (gray values of all pixels in the ROI of the first response in the 250 msec ISI 531,664±45,695, in the 500 msec ISI 543,453±72,130, and in the 1,000 msec ISI 624,980±11,703) were statistically tested and

found not to be statistically different (RM ANOVA df=31, F=0.39, p=0.7). That is, the density of the ITC following the first stimulus was equivalent across the three different ISIs, suggesting that the initial activation of the M50 was equivalent across all ISIs. In addition, we performed IOD measures on the 40-70 msec latency region following the first stimulus in the No Response condition (n=8, 174,910±27,093 gray values) and compared this ITC density to the one following the first stimulus in the Response condition (n=8, 179,610±34,758 gray values). There was no statistically significant difference between these measures (RM ANOVA df=15, F=0.06, p=0.8), suggesting that the density of the ITC following the first stimulus of a pair was not changed by the subsequent requirement to respond in the go-no go Response task, compared to that in the same-different No Response condition.

M50 Habituation to repetitive stimuli

The response after the second stimulus as a percent of the response after the first was calculated for each subject's M50 IC. The average percent habituation for the 14 subjects studied at the 250 msec ISI was 13±5 %, while at the 500 msec ISI it was 66±10 %, and at the 1,000 msec ISI it was 76±14 %). Figure 3A shows that, in relation to the response to the first stimulus (100 % for each ISI), the average percent habituation at the three ISIs tested progressively decreased, representing a gradual recovery curve of the response as the ISIs increased. In addition, the percent habituation of the ITC for different frequencies is plotted for 0-10, 10-20, 20-30, 30-40 and >40 Hz. The recovery curves for the individual frequency ranges suggest that lower frequencies recovered faster than higher frequencies. Statistical comparison of the percent habituation at the three ISIs showed that there was a significant difference in percent habituation across ISIs (RM ANOVA df=31, F=14.5, $p<0.001$). Post hoc analysis (Scheffe test) showed that the percent habituation at the 250 msec ISI was significantly lower than that at the 500 msec and 1,000 msec ISIs ($p<0.01$).

M50 Response vs No Response habituation

ERSPs were present in a minority of cases in the No Response (3/8) and Response (3/8) conditions. In only one case (see below) was the ERSP of a density similar to that for the ITCs. Otherwise, it was of considerably lower density, but because they were so few in number (n=3), statistical comparisons were not made. As described above, the density of the ITC following the first stimulus in the No Response trials (250 msec ISI) did not differ from that after the first stimulus in the Response trials (also using a 250 msec ISI). This suggests that the density of the response to the initial stimulation was not affected by the requirement to respond. When the ITC density after the second stimulus in the Response condition was compared to that following the No Response condition, there was a trend towards a decrement in habituation. That is, the habituation (response to the second stimulus as a percent of the response to the first) described above at the 250 msec ISI in the No Response condition was 23±4 %, while that at the 250 msec ISI during the Response condition was almost double at 41±7 % (RM ANOVA df=15, F=3.99, p=0.09). This suggests that the requirement to respond led to a numerical (statistically insignificant) decrease in the habituation to repetitive stimuli, at least at the 250 msec ISI.

Figure 4 shows a representative ITC plot of a M50 source in the No Response (Fig. 4A) and in the Response (Fig. 4B) condition. In this case, the ITC induced by the first and second stimuli appeared to be of increased density in the Response condition, although there was no statistical difference between the mean ITC density in the group (n=8) following the first stimulus across the two conditions, and only a numerical trend towards increased mean ITC density in the group (n=8) after the second stimulus in the Response condition. The ICs shown in this figure also represent the only case in which a significant ERSP was present in both No Response and Response conditions at 40-70 msec latency.

Primary auditory cortex (Pa)

Localization of the primary auditory cortex was based on determining a magnetic source on the inflated maps. All of the localization maps were first searched for activation in the primary auditory cortex on the posterior aspect of the superior temporal lobe. Of the 14 subjects recorded at the 250 msec ISI, all but one showed at least one map with activation of the primary auditory cortex. Of the remaining 13 subjects, all but 4 showed activation sites in both left and right primary auditory cortices, and the others showed activation only on one auditory cortex. The corresponding ERSP and ITC plots of these sources were then searched for activation at 20-30 msec latency after the first and/or second stimulus of a pair. Similar to the patterns seen at the 40-70 msec latency, the ERSP plots showed that only a minority of subjects (5/14) exhibited activation, while the ITC plots showed activation at a 20-30 msec latency following either the first (10/13) or second (9/13) stimulus of a pair. In fewer cases (5/13) activation was present after both the first and the second stimuli.

Of the 12 subjects recorded at the 500 msec ISI, all but 4 showed at least one inflated map with activation of the primary auditory cortex, with 4/8 showing activation on both left and right auditory cortex and 4/8 showing activation only on one side. The corresponding ITC plots showed activation at a 20-30 msec latency following either the first (7/8) or the second (3/8) stimulus of a pair. Of the 6 subjects recorded at the 1,000 msec ISI, 5/6 subjects showed activation on both left and right auditory cortices, and 1/6 did not show auditory cortex activation. Again at the 1,000 msec ISI, the ITC plots showed activation at a 20-30 msec latency following either the first (4/5) or second (4/5) stimulus of a pair.

Figure 5 shows localization of different ICs on the left and right auditory cortices on inflated maps in a representative subject. The ITC plots for the corresponding ICs showed that the ITC at these sources was present at the 20-30 msec latency after the first and/or second stimulus of a pair, denoting activation of the primary auditory cortex at the latency of the Pa potential (20-30 msec). This figure was chosen because it also shows activity at a 40-70 msec latency in the case of the left auditory cortex localization (Fig. 5A, IC23) in this subject, although not in the right auditory cortex (Fig 5B, IC35). There was ITC activation at the 40-70 msec latency after the first stimulus in ICs of inflated maps showing auditory cortex localization in either left (9/14) or right side (4/14). ITC activation was present at 40-70 msec only after the second stimulus (and not the first), or was increased in density after the second stimulus compared to the first, in some of these cases on the left (5/9) and on the right (2/4) auditory cortex. Such activity did not meet the M50 criterion of habituation to repetitive stimulation. However, in 4/9 of these cases on the left and 2/4 cases on the right, there was ITC activation at 40-70 msec after the first stimulus that also decreased in density after the second. While this met the criterion for M50 habituation, none of these ICs had comparable ITC densities to the ICs meeting the criteria for M50 sources. Nevertheless, in a minority of cases, ITC activation that habituated to repetitive stimulation was occasionally present in auditory cortex sources.

Oscillatory activation

In a number of ITC plots, oscillatory activation was present, persisting hundreds of milliseconds. Such oscillations were evident in 4/14 M50 sources at the 250 msec ISI (Mean ±SE, Frequency 22±4 Hz), 6/12 M50 sources at the 500 msec ISI (22±2 Hz), and in 3/6 M50 sources at the 1,000 msec ISI (23±2 Hz). Such oscillations were less frequently observed in primary auditory cortex sources (2/14 at 250 msec, 2/12 at 500 msec, 3/6 at 1,000 msec). In the No Response condition, 5/8 plots showed oscillations in the ITC after the first stimulus, with only 2/5 showing oscillations after the first and second stimulus (21±1 Hz). However, in 7/8 plots in the Response condition there was oscillatory ITC after the first stimulus, and 4/8 showed oscillations after the first and second stimuli (22±1 Hz). An example of such oscillatory activation is shown in figure 4 for both No Response and Response conditions for a M50 source.

These oscillations were most evident as recurrent activation in the 0-10 Hz band (across the top of each ITC plot). These oscillations were sometimes present in advance of the first stimulus and persisted until after the second stimulus. The ITC plot in figure 1C shows activation peaking at ~50 msec after the first stimulus followed by recurrent activation until the second stimulus. The ITC plot in figure 4 for the No Response (Fig. 4A) and Response (Fig. 4B) conditions shows oscillatory activation at a frequency of 20 Hz, with more pronounced density in the Response condition. An example of oscillatory activation, characteristically less pronounced than for M50 sources, is also shown for a primary auditory cortex source in Figure 5A.

Discussion

Briefly, our results showed that each subject exhibited localization of a source on inflated maps for primary auditory evoked responses in the region of the auditory cortex at a 20-30 msec latency. However, responses at a 40-70 msec latency that also decreased following the second stimulus of a pair, detected as ITC activation after each stimulus, were generally not localizable to the auditory cortex, rather showing multiple sources, usually including the frontal lobes. That is, the M50 response, the presumed equivalent of the P50 midlatency auditory evoked potential, which shows habituation to repetitive stimulation, was not primarily localized to the auditory cortex, and may represent non-auditory activation. Measures of ERSP density showed little consistency across subjects and ISIs. Measures of ITC density were more consistent and revealed that the density of ITC at M50 sources was similar following the first stimulus at any of the ISIs used, suggesting equivalent initial activation of the system with the first stimulus of a pair. Similarly, in the No Response and Response conditions, the density of ITC at M50 sources was similar following the first stimulus, again suggestive of equivalent and consistent initial activation of the system. However, habituation to repetitive stimulation was evident in the decrease in density of ITC at these sources induced by the second stimulus of each pair, especially at the 250 msec ISI. Finally, M50 sources elicited oscillatory ITC that lasted hundreds of milliseconds, and were especially prominent in the Response condition.

M50 Localization

Rather than assuming that M50 sources would be localized in and around the primary auditory cortex on the superior temporal gyrus, we determined localization from a) the greatest activation at ~50 msec latency that would b) habituate to repetitive stimulation (see Figure 2). Recent EEG recordings with subdural electrodes revealed that paired stimuli induced habituating responses at ~50 msec latency in only a minority of subjects (6/24), and only in temporo-parietal and prefrontal cortex, but not in primary auditory cortex (Grunwald et al., 2003). Previous MEG studies have measured only temporal lobe channels and averaged them to estimate M50 sources (Clementz et al., 1997), while some modeled equivalent current dipoles, averaged them (Hanlon et al., 2005), and localized them to the temporal lobe by modeling different dipoles for activation after the first compared to the second stimuli (Thoma et al., 2005), all using only a single ISI, i.e. all assumed a primary auditory cortex source and none generated a recovery curve using different ISIs.

The present analysis used ICA to localize sources without averaging, did not assume a superior temporal gyrus source and used three ISIs to generate a recovery curve for the same response (Figure 3). Our findings suggest that M50 sources were present in all subjects and showed diffuse localization usually including frontal lobes. The consistency of the density of activation following the first stimulus of a pair lends further credence to the fact that it was the same phenomenon that was measured across ISIs in each subject. However, in a minority of cases, there was activation at ~50 msec latency at primary auditory cortex sources, suggesting M50-like activation, but not as great as that seen in frontal lobe sources. We suspect that such

responses, seen only in a limited population, may have led others to localize the M50 to primary auditory cortex. This also suggests that auditory stimuli do also lead to activation of this region, in addition to frontal/diffuse regions, at least in a minority of subjects. A primary auditory cortex source (presumed to be the equivalent of the Pa potential) on the superior temporal gyrus was present in all but one of our subjects, usually in each hemisphere. The magnetic equivalent of the Pa potential, then, was consistently manifested in primary auditory cortex at ~25 msec latency (Figure 5).

ERSP and ITC activation

Our results suggest that the paired stimulus paradigm that led to activation of M50 sources using the criteria outlined did not induce significant and consistent changes in ERSP. Rather, only the ITC reflected consistent activation at ~50 msec latency and only the ITC showed a decrement with repetitive stimulation at the same latency. Moreover, only the ITC revealed a recovery curve for this effect at increasing ISIs (see Figure 3). This suggests that the activation induced essentially led to phase resetting, in keeping with an oscillatory model of function. The M50 may thus represent a process leading to an increase in phase concentration of oscillations. If this is the case, considerations limited to ERSP contributions may not reveal the true nature of M50 manifestation.

We speculate that the M50 represents a phase resetting induced by the stimulus on ongoing oscillations. This is in keeping with a model of sensory function based on thalamocortical oscillations, with the primary afferent (specific thalamic) pathways representing the content of sensory experience and the intralaminar diffuse (non-specific thalamic) pathways representing the context of sensory experience (Llinas 2001). The former may be reflected in the primary cortical (Pa) response, while the latter may be represented by intralaminar diffuse (P50/M50) activation. This is in keeping with the proposed origin of the P50 potential as a preattentional/arousal-related, non-auditory response (Erwin and Buchwald, 1986a, b). Such activation would be characterized by rapid habituation in the absence of significant changes in the initial response, as observed in the present studies. That is, while primary cortical activation is consistent in modulating ongoing oscillations, habituation of the M50 would provide a change in phase resetting with repetitive stimulation.

Response vs No Response

Since there were no significant increases in the average density of the ITC (although there was an increase in individual cases, see e.g. Figure 4) in the Response vs No Response condition, it can be concluded that the subsequent need to respond did not influence the overall level of coherence prior to the response. We should note that the No Response condition was not entirely passive as it required a same-different discrimination, so that some level of attention was required. Future studies will need to assess more complex tasks to determine if the level of attention required is related to the density of ITC activation. In the Response condition, there was a trend towards decreased habituation, indicative of a greater load in the same different, go-no go discrimination. However, these data do confirm the frontal lobe localization of M50-like sources (Figure 4).

Oscillations

Although oscillatory activation in the low frequency band (0-10 Hz) appeared greater in the Response condition, it was also present in the No Response condition, regardless of ISI. While such oscillatory activation was more often found in M50 sources (Figure 4), it could also be seen in some primary auditory cortex sources, although of lower density (Figure 5). The frequency of oscillations was measured at ~20 Hz across the three ISIs tested and ~20 Hz in the No Response and Response trials. These oscillations occurred only during the delivery of the paired stimuli and not across the entire sampling period. The presence of such oscillations

at the low frequency band suggests that the paired stimulus task was superimposed on a secondary state of coherent activation that may have expectation as a component since oscillations sometimes preceded the first stimulus.

In summary, these preliminary studies suggest that the paired stimulus paradigm can be used to detect localization of M50 responses and habituation to repetitive stimulation. The data point to a non-auditory, possibly arousal or preattentional, role for the M50.

Acknowledgements

Supported by NYU GCRC grant RR00096 and UAMS center grant RR020146.

References

Adler LE, Pachtman E, Franks RD, Pecevich RD, Waldo MC, Freedman R. Neuropsychological evidence for a defect in neuronal mechanisms involved in sensory gating in schizophrenia. Biol Psychiat 1982;17:639–654. [PubMed: 7104417]

Boop FA, Garcia-Rill E, Dykman R, Skinner RD. The P1: insights into attention and arousal. Pediat Neurosurg 1994;20:57–62.

Boutros NN, Belger A. Mid-latency evoked potential attenuation and augmentation reflect different aspects of sensory gating. Biol psychiat 1999;45:917–922. [PubMed: 10202580]

Brown GD, Yamada S, Sejnowski TJ. Independent component analysis at the neural cocktail party. Trends Neurosci 2001;24:54–63. [PubMed: 11163888]

Buchwald JS, Erwin R, Van Lanker D, Cummings JL. Midlatency auditory evoked responses: P1 abnormalities in adult autistic subjects. Electroenceph clin Neurophysiol 1992;84:164–171. [PubMed: 1372231]

Clementz BA, Blumfeld LD, Cobb S. The gamma band response may account for poor P50 suppression in schizophrenia. NeuroReport 1997;8:3889–3893. [PubMed: 9462461]

Delorme A, Makeig S. EEGLAB: an open source toolbox for analysis of single-trial EEG dynamics including independent component analysis. J Neurosci Methods 2004;134:9–21. [PubMed: 15102499]

Edgar JC, Huang MX, Weisend MP, Sherwood A, Miller GA, Adler LE, Canive JM. Interpreting abnormality: an EEG and MEG study of P50 and the auditory paired-stimulus paradigm. Biol Psychol 2003;65:1–20. [PubMed: 14638286]

Erwin RJ, Buchwald JS. Midlatency auditory evoked responses: differential effects of sleep in the human. Electroenceph clin Neurophysiol 1986a;65:383–392. [PubMed: 2427329]

Erwin RJ, Buchwald JS. Midlatency auditory evoked responses: differential recovery cycle characteristics. Effects of sleep in the human. Electroenceph clin Neurophysiol 1986b;64:417–423. [PubMed: 2428592]

Fischl B, Sereno MI, Dale AM. Cortical surface-based analysis. II: Inflation, flattening, and a surface-based coordinate system. NeuroImage 1999;9:195–207. [PubMed: 9931269]

Fischl B, Salat DH, Busa E, Albert M, Dieterich M, Haselgrove C, van der Kouwe, Killiany R, Kennedy D, Klaveness S, Montillo A, Makris N, Rosen B, Dale AM. Whole brain segmentation: automated labeling of neuropanatomical structures in the human brain. Neuron 2002;33:341–355. [PubMed: 11832223]

Funetemilla L, Marco-Pillares J, Grau C. Modulation of spectral power and of phase resetting of EEG contributes differentially to the generation of auditory event-related potentials. NeuroImage 2006;30:909–916. [PubMed: 16376575]

Garcia-Rill, E.; Skinner, RD. The sleep state-dependent P50 midlatency auditory evoked potential. In: Lee-Chiong, TL.; Sateia, MJ.; Carskadon, MA., editors. Sleep Medicine. Hanley & Belfus, Inc; Philadelphia: 2002.

Garcia-Rill E, Skinner RD, Clothire J, Dornhoffer J, Uc E, Fann A, Mamiya N. The sleep state-dependent midlatency auditory evoked P50 potential in various disorders. Thal Rel Syst 2002;2:9–19.

Godey B, Schwartz D, de Graff JB, Chauvel P. Liegeois-Cahuvel C. Neuromagnetic source localization of auditory evoked fields and intracerebral evoked potentials: a comparison of data in the same patients. Clin Neurophysiol 2001;112:1850–1859. [PubMed: 11595143]

Goff WR, Williamson PD, Van Gilder JC, Allison T, Fisher TC. Neural origins of long latency evoked potentials recorded from the depth and from the cortical surface of the brain in man. Prog Clin Neurophysiol 1980;7:126–145.

Grunwald T, Boutros NN, Pezer N, van Oertzen J, Fernandez G, Elger CE. Neuronal substrates of sensory gating within the human brain. Biol Psychiat 2003;53:511–519. [PubMed: 12644356]

Hanlon FH, Miller GA, Thoma RJ, Irwin J, Jones A, Moses SN, Huang M, Weisend MP, Paulson KM, Edgar JC, Adler LE, Canive JM. Distinct M50 and M100 auditory gating deficits in schizophrenia. Psychophysiol 2005;42:417–427.

Inui K, Okamoto H, Miki K, Gunji A, Kakigi R. Serial and parallel processing in the human auditory cortex: a magnetoencephalographic study. Cerebral Cortex 2006;16:18–30. [PubMed: 15800024]

Kevanishvili Z, von Specht H. Human auditory evoked potentials during natural and drug-induced sleep. Electroenceph clin Neurophysiol 1979;47:280–288. [PubMed: 90599]

Knight RT, Staines WR, swick D, Chao LL. Prefrontal cortex regulates inhibition and excitation in distributed neural networks. Acta Psychologia 1999;101:159–178.

Llinas, RR. From neurons to self. MIT Press; Cambrige, MA: 2001. I of the Vortex.

Llinas R, Ribary U, Jeanmonod D, Kronberg E, Mitra PP. Thalamocortical dysrhythmia: a neurological and neuropsychiatric syndrome characterized by magnetoencephalography. Proc Natl Acad Sci 1999;96:15222–15227. [PubMed: 10611366]

Makela JP, Hamalainen M, Hari R, McEvoy L. Whole-head mapping of middle-latency auditory evoked magnetic fields. Electroenceph clin Neurophysiol 1994;92:414–421. [PubMed: 7523085]

Makeig S, Jung TP, Bell AJ, Ghahremani D, Sejnowski TJ. Blind separation of auditory event-related brain responses into independent components. Proc Natl Acad Sci 1997;94:10979–10984. [PubMed: 9380745]

Makeig S, Westerfield M, Jung TP, Enghoff S, Townsend J, Courchesne E, Sejnowski TJ. Dynamic brain sources of visual evoked responses. Trends Neurosci 2002;25:387–389. [PubMed: 12127748]

Onitsuka T, Ninomiya H, Sato E, Yamamoto T, Tashiro N. Differential characteristics of the middle latency auditory evoked magnetic responses to interstimulus intervals. Clin Neurophysiol 2003;114:1513–1520. [PubMed: 12888035]

Pekkonen E, Jaaskelainen IP, Kaakkola S, Ahveninen J. Cholinergic modulation of preattentive auditory processing in aging. NeuroImage 2005;27:387–392. [PubMed: 15921933]

Reite M, Teale P, Zimmerman J, Davis K, Whalen J. Source localization of a 50 ms latency auditory evoked field potential. Electroenceph clin Neurophysiol 1988;70:490–498. [PubMed: 2461283]

Skinner RD, Rasco LM, Fitzgerald J, Karson CN, Matthew M, Williams DK, Garcia-Rill E. Reduced sensory gating of the P1 potential in rape victims and combat veterans with posttraumatic stress disorder. Dep Anxiety 1999;9:122–130.

Teo C, Rasco L, Al-Mefty K, Skinner RD, Garcia-Rill E. Decreased habituation of midlatency auditory evoked responses in Parkinson's disease. Movement Disord 1997;12:655–664. [PubMed: 9380045]

Thoma RJ, Hanlon FM, Moses SN, Ricker D, Huang M, Edgar C, Irwin J, Torres F, Weisend MP, Adler LE, Miller GA, Canive JM. Schiz Res 2005;73:311–318.

Uc E, Skinner RD, Rodnitzky L, Garcia-Rill E. The midlatency auditory evoked potential P50 is abnormal in Huntington's Disease. J Neurol Sci 2003;212:1–5. [PubMed: 12809992]

Vaughan HG, Ritter W. The sources of the auditory evoked responses recorded from the human scalp. Electroenceph clin Neurophysiol 1970;28:360–367. [PubMed: 4191187]

Williamson PD, Goff WR, Allison T. Somato-sensory evoked responses in patients with unilateral cerebral lesions. Electroenceph clin Neurophysiol 1970;28:566–575. [PubMed: 4192832]

Wood CD, Wolpaw JR. Scalp distribution of human auditory evoked potentials. Part II. Evidence for overlapping sources and involvement of auditory cortex. Electroenceph clin Neurophysiol 1982;54:25–38. [PubMed: 6177515]

Woods DL, Knight RT, Neville HJ. Bitemporal lesions dissociate auditory evoked potentials and perception. Electroenceph clin Neurophysiol 1984;57:208–220. [PubMed: 6199182]

Yoshiura T, Ueno S, Iramina K, Masuda K. Source localization of middle latency auditory evoked magnetic fields. Brain Res 1995;703:139–144. [PubMed: 8719625]

Yvert B, Fischer C, Bertrand O, Pernier J. localization of human supratemporal auditory areas from intracerebral auditory evoked potentials using distributed source methods. NeuroImage 2005;28:140–153. [PubMed: 16039144]

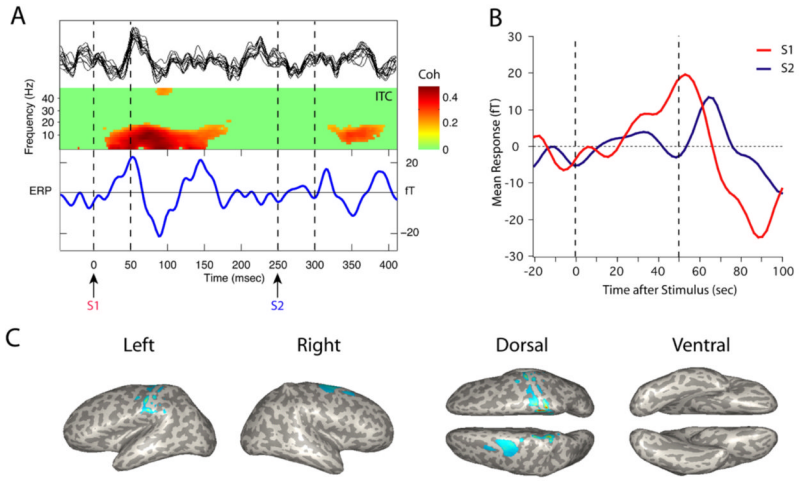

Figure 1. Independent Component showing activation at ~50 msec that habituated after the second stimulus

A. The superimposed individual waveforms shown at the top are from a sensor in the posterior frontal lobe showing a response after the first stimulus and a much reduced response after the second. Below that are the inter-trial coherence (ITC) image and event related potential (ERP) showing the strength of phase-locking of the MEG signal for an independent component for two stimuli with an ISI of 250 msec. The ITC showed a band of increased coherence ~50-100 msec after the first stimulus in the alpha and beta frequency ranges. This phase locking contributes to the event related potential (ERP) shown below the ITC. The false color scale indicating synchronization at positive values (red) and desynchronization at negative values (blue) (green in image indicates p<.001). **B.** Superposition of response following the first stimulus S1 (red) and the second S2 (blue) showing decreased responsiveness after the second, i.e. habituation. **C.** Localization of independent components in A. Inflated maps showing localization of the source with distributed activation at several fronto-parietal sites.

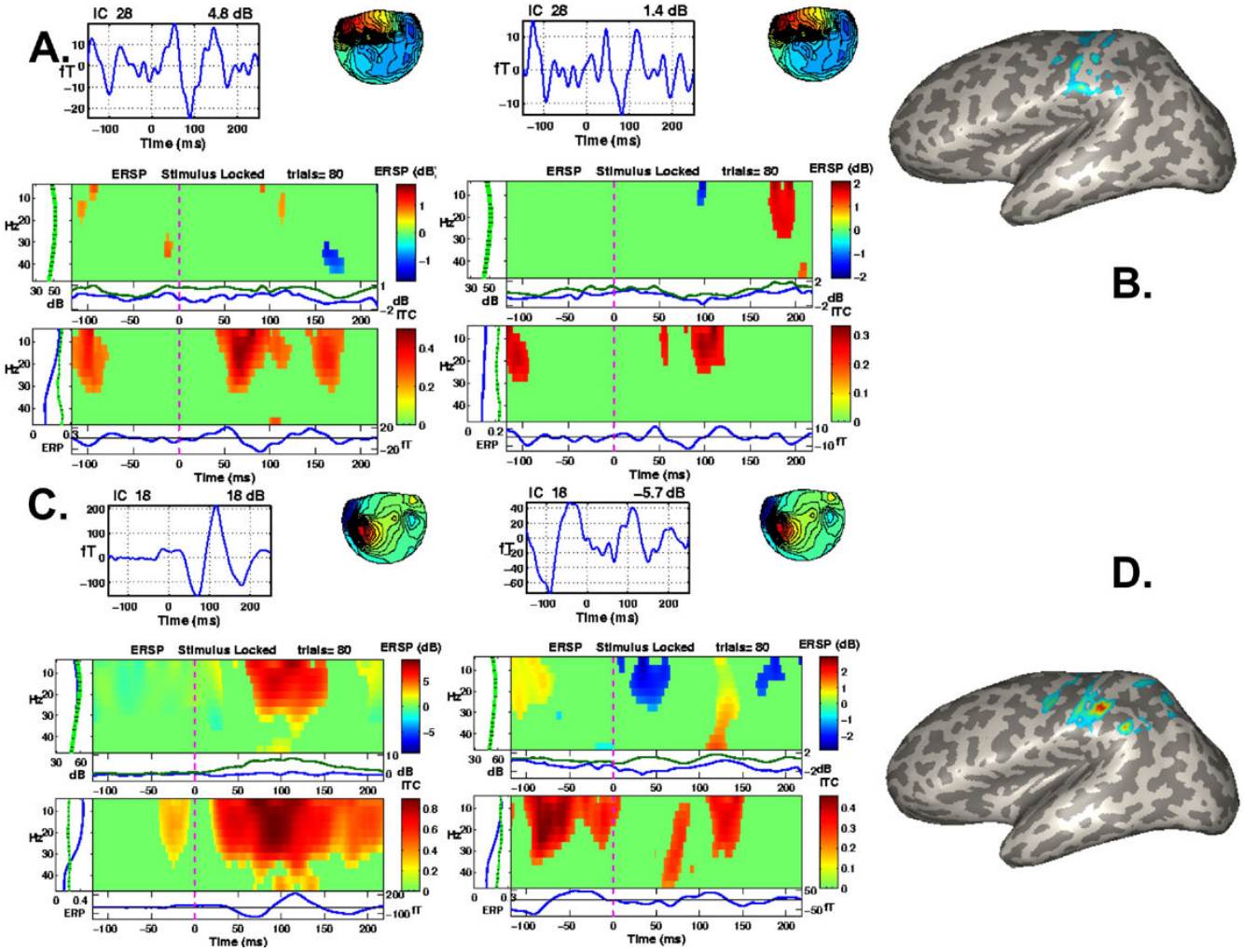

Figure 2. Independent Components showing activation at ~50 msec that habituate after the second stimulus

A. Left side. Activation at IC28 in a representative subject showing a plot of the evoked average magnetic response after the first stimulus. Right, distribution of the magnetic flux over the sensors. Below the fT plot is a plot of the ERSP induced at this source before (175 msec before the stimulus) and after (225 msec after) the first stimulus (vertical dashed line), showing little activation at ~50 msec. The left axis shows the activation by frequency between 0 and 50 Hz, while the right axis shows the false color scale indicating synchronization at positive values (green to red) and desynchronization at negative values (green to blue). The ITC plot below the ERSP plot also shows activation by frequency on the left axis but on the left axis is shown the density of activation from none (green) to greatest (black). The ITC showed significant activation at ~50 msec latency. **Right side.** Activation of the same IC after the second stimulus of a pair, in this case at the 250 msec ISI, denoted by the vertical dotted line. The fT plot shows a plot of the evoked response after the second stimulus. The ERSP plot shows no activation at ~50 msec after the second stimulus, while the ITC plot shows a lower level of activation at ~50 msec than after the first stimulus. **B.** Inflated map of the source of IC28 showing activation at several fronto-parietal sites. **C. Left side.** Activation at IC18 in another subject showing the fT plot evoked response, activation of the ERSP plot at a latency ~60 msec, but considerable activation of the ITC plot at ~50 msec. Note the oscillatory activation recurring about every

50 msec. **Right side.** Activation of the same IC after the second stimulus of a pair, in this case at the 250 msec ISI, denoted by the vertical dotted line. The fT plot shows a plot of the evoked response after the second stimulus. The ERSP plot shows some difference (desynchronization) at ~25-50 msec after the second stimulus, while the ITC plot shows a lower level of activation at ~50 msec than after the first stimulus. **D.** Inflated map of the source of IC18 showing activation at several frontal and parietal lobe sites.

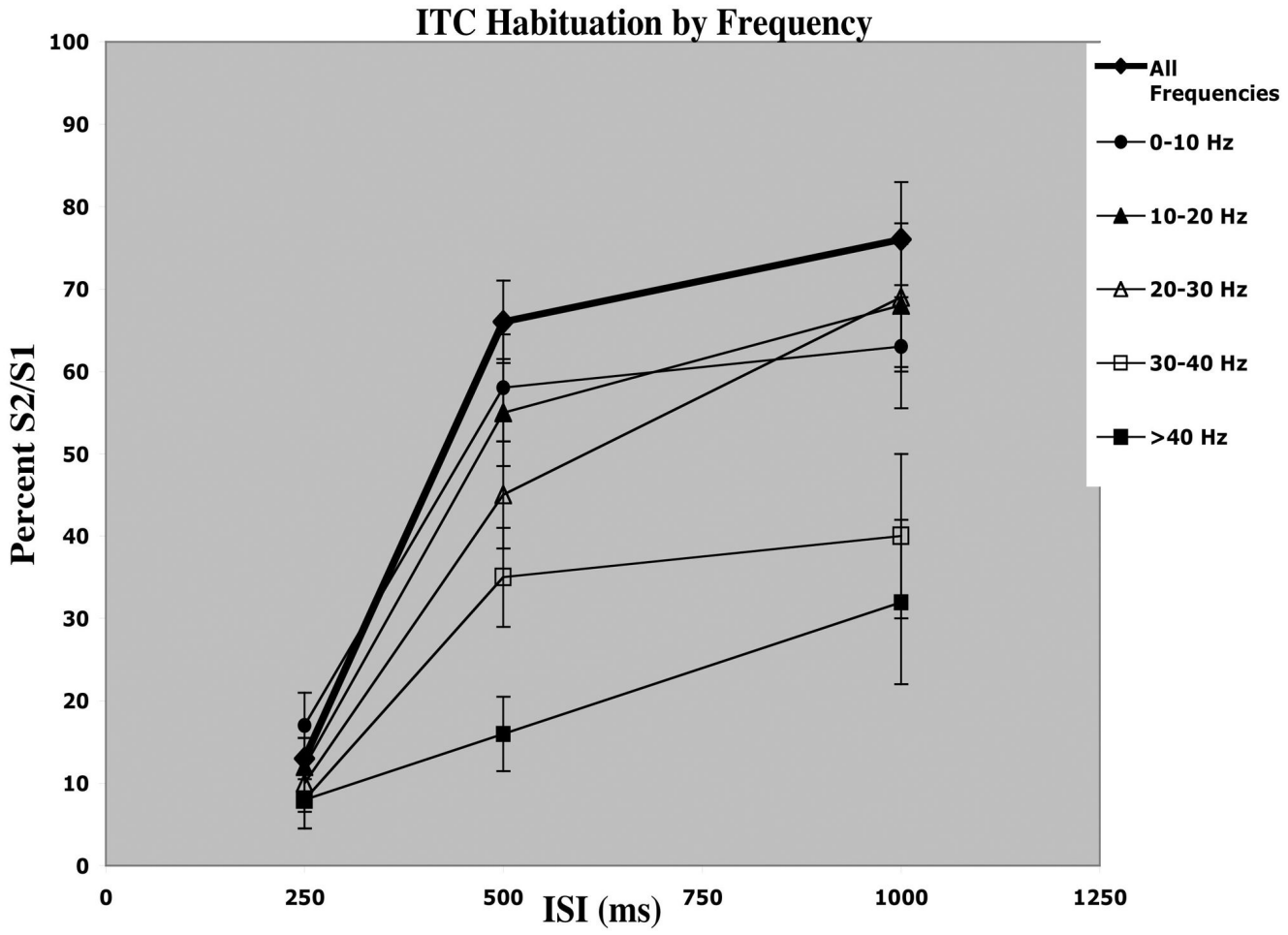

Figure 3. Recovery curve of M50 at various ISIs

The average (±SE) percent habituation of the M50 ITC density for all subjects is plotted such that the response to the first stimulus of a pair at any ISI was designated as 100%. The ITC density for all frequencies is plotted as a thick black line with filled diamonds. Individual frequency ranges are plotted as 0-10 Hz filled circles, 10-20 Hz filled triangles, 20-30 Hz open triangles, 30-40 Hz open squares, and over 40 Hz as filled squares. The percent habituation at the 250 msec ISI was 13±5 %, while at the 500 msec ISI it was 66±10 %, and at the 1,000 msec ISI it was 76±14 %. Percent habituation at the 250 msec ISI was significantly lower than that at the 500 msec and 1,000 msec ISIs ($p<0.01$). The habituation of the individual frequency ranges followed the same trend as the overall recovery curve. However, habituation was greater at the higher frequencies.

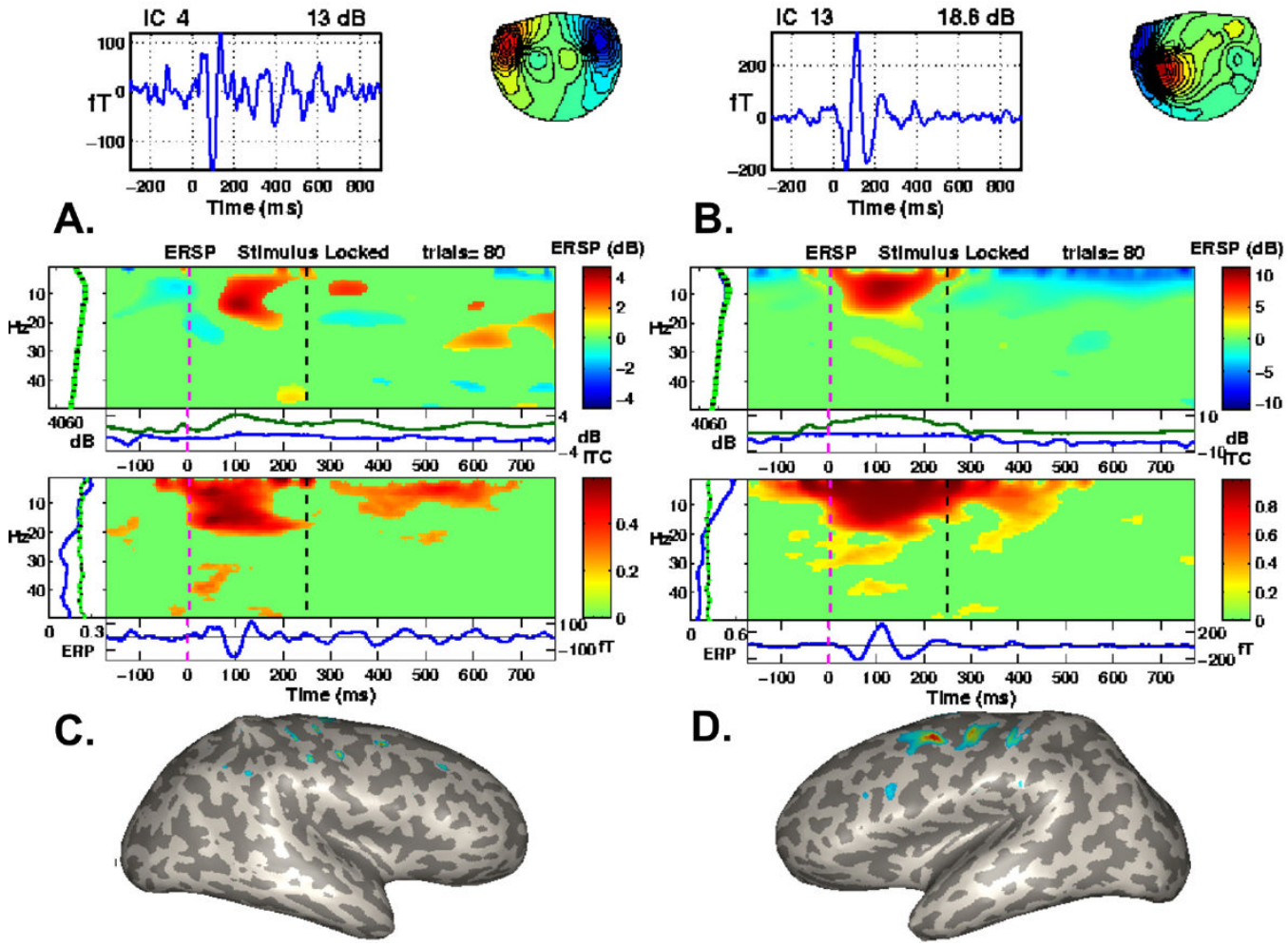

Figure 4. No Response vs Response activation

A. A source (IC4) in a subject during the No Response condition showing a response in the fT plot and after the first (vertical pink dotted line) and second (vertical dotted line) stimuli. Note the activation of the ITC following the first stimulus was reduced after the second stimulus, although both stimuli induced oscillatory activation. **B.** A source (IC13) in the same subject during the Response condition showing a response in the fT plot and after the first (vertical pink dotted line) and second (vertical dotted line) stimuli. Note the increased activation of the ITC following the second stimulus was reduced, but also increased compared to the No response condition, although both stimuli induced oscillatory activation. **C.** Inflated map of the source of IC4 shown in A, exhibiting activation at several frontal and parietal lobe sites. **D.** Inflated map of the source of IC13 shown in B, exhibiting activation at several frontal lobe sites.

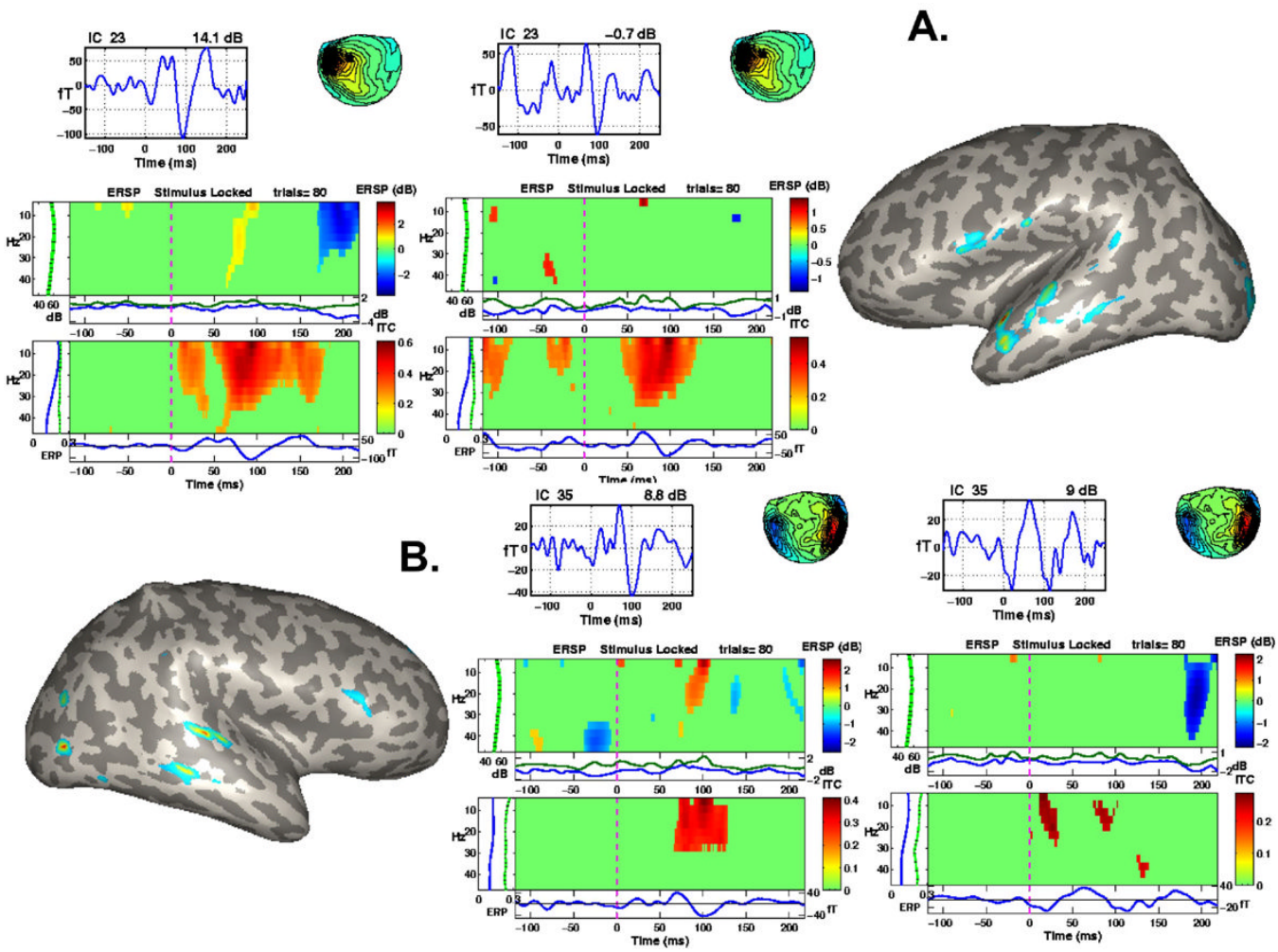

Figure 5. Independent Components showing activation at ~25 msec

A. A source (IC23) in a subject during the 250 msec ISI showing the response in the fT plot, and the responses after the first (left ERSP and ITC plots) and second (right ERSP and ITC plots) stimuli. Note the activation of the ITC following the first stimulus was present at ~25 msec (as well as at ~50 msec), but absent at ~25 msec after the second stimulus (and reduced after the second stimulus at ~50 msec latency), and both stimuli induced oscillatory activation. The inflated map on the right shows the localization of a source on the superior temporal gyrus, as well as other parts of the temporal and frontal lobes, denoting activation of the left primary auditory cortex. **B.** A source (IC35) in a subject during the 250 msec ISI showing a response in the fT plot, and the responses after the first (left ERSP and ITC plots) and second (right ERSP and ITC plots) stimuli. Note the lack of activation of the ITC following the first stimulus at ~25 msec (as well as at ~50 msec), but present at ~25 msec after the second stimulus (and absent after the second stimulus at ~50 msec latency), and both stimuli induced oscillatory activation. The inflated map on the left shows the localization of a source on the superior temporal gyrus, as well as other parts of the temporal, occipital and frontal lobes, denoting activation of the right primary auditory cortex.